Design and Mechanical Tests of FRP Pipe with Bamboo and Veneer Layer

Hongguang Liu,* Bin Luo, Shijie Shen, and Li Li

Pipes that are light in weight are necessary for convenience and to reduce the cost of transportation and installation. A new design of glass fiber reinforced plastic (FRP) pipe with a bamboo and veneer layer is presented in this paper. The core layer of the sandwich structure of the pipe wall is made of bamboo and veneer, and the inner and outer layers are FRP. Range analysis and variance analysis of orthogonal experiments were conducted to investigate the effect of fiber stress, winding angle, and core material on the mechanical performance of the pipes subjected to shearing and parallel-plate loading tests. The results indicated that the new design of FRP pipe with a bamboo and veneer layer was feasible, and the pipe had better mechanical performance with a fiber stress of 300 N, a winding angle of 30°, and a core material of bamboo. Core material was the most influential factor in mechanical performance. The average density of pipes was 0.94 g/cm^3, approximately half that of the glass fiber reinforced plastic mortar (GRPM) pipes. The FRP pipe offered advantages in terms of weight savings and improved mechanical performance, and it showed a great application potential for the future.

Keywords: Glass fiber reinforced plastic pipe; Glass fiber reinforced plastic mortar pipe; Bamboo and veneer; Filament winding; Core material; Sandwich structure

Contact information: College of Materials Science and Technology, Beijing Forestry University, No. 35 Tsinghua East Rd, Haidian District, Beijing, 100083, P. R. China; Corresponding author: Hongguang Liu, Email:bjfuliuhg@163.com

INTRODUCTION

In recent decades, glass fiber reinforced plastic (FRP) pipes have been commonly used in many engineering applications including the storage and transfer of oil and gas, municipal piping, power plants, irrigation, and potable water transmission systems. Their unique characteristics, including that they are light in weight, high in strength and stiffness, high in corrosive resistance, have smooth internal surfaces, and have easy joining systems, have enabled their diverse utilization. Fiber reinforced plastic pipes have been the main competitors of traditional concrete, steel, and asbestos pipes in the aforementioned fields of applications (Chen 2012; Rafiee and Amini 2015).

Fiber-reinforced plastic pipes are most commonly manufactured using the filament winding method (Fig. 1). Continuous fibers or belts pass through a resin bath and are then applied to a rotating cylindrical mandrel *via* a travelling trolley that moves from one end to the other. The use of continuous fibers ensures the evenness in the direction of the fiber arrangement, and the use of cylindrical mandrel ensures evenness in the inside diameters of pipes. This procedure in the industrial production line is commercially called the filament winding process (Rafiee and Amini 2015).

Different studies have examined the manufacture process, mechanical properties, and applications of FRP pipes. Yang (2008) developed a numerical method to study the

thermal cure process of filament winding composite cylinder based on the Springer thermal chemical model. Xu *et al.* (2009) presented a new *in situ* modeling process for FRP pipes. The method of heating the internal metal mandrel of the pipe was adopted to realize the curing of the pipe. Kong and Kong (2010, 2011) described the design principal and basic methods of thermosetting composites, emphatically discussed the essence, harm and preventive measures of temperature lag and overshoot of thick composite laminates during curing and introduced three simulated test methods of cure schedule. Mehmet and Ramazan (2012) examined the effect of seawater immersion on the impact behavior of FRP pipes. Krishnan *et al.* (2015) investigated the effects of the winding angle on the behavior of FRP pipes under multiaxial cyclic loading. Rafiee and Amini (2015) carried out experimental and theoretical studies that predicted the functional failure pressure of FRP pipes subjected to hydrostatic internal pressure.

When pipes of relatively large diameter were required in actual use, the wall thickness had to increase to fulfil the requirement of pipe stiffness and to bear high pressures. From the point of view of stress analysis, under external loading, normal stress of the center area of wall was small, shearing stress was higher than other areas, and the shearing stress of all areas was small. Thus, the center area of the wall was in a low stress state. As a consequence, the FRP pipe producers incorporated an impregnated sand filler layer in between the FRP plies to enhance the stiffness of the pipe as an economical solution, instead of increasing thickness by adding redundant FRP layers. Presently, silica sand is commonly used as a core material to manufacture glass fiber reinforced plastics mortar (GRPM) pipes. These pipes are sandwich-type composites that use polymer mortar and have a relatively high rigidity at the core of the pipe walls, and use FRP with a high tensile strength for the inner and outer pipe walls.

Many investigations have been conducted on the technological process and mechanical behavior of GRPM pipes. Qin (1996) introduced the sandwich wall structure of GRPM pipes and analyzed the technological process and parameters of GRPM pipes. Kaveh and Farid (2011) investigated the influence of the structural parameters that significantly impacted the characteristic behavior and pressure capacity of sandwich pipe systems and developed three simplified practical equations, capable of evaluating the pressure capacity of sandwich pipes having various intra-layer mechanisms and material configurations. Arjomandi and Taheri (2012) investigated the behavior of sandwich pipes subject to pure bending, which is one of the governing loading conditions for offshore pipelines. Yang *et al.* (2013) presented some main points of production quality control according to the technological process of GRPM pipes and suggested some solutions for usual quality problems. Rafiee and Reshadi (2014) carried out simulation and analysis of the functional failure in composite pipes subjected to internal hydrostatic pressure. Wang *et al*. (2014) analyzed ring stiffness related to concepts and basic methods of design and testing and provided a method of calculating finite element method (FEM) ring stiffness. Li *et al*. (2015) designed and manufactured a series of composite foam sandwich pipes with different parameters and investigated the influence factors that experimentally determine the axial compressive performances of the tubes. Sburlati and Kashtalyan (2016) investigated sandwich pipes with two thin functionally graded interlayers between the core layer and inner/outer pipes in the context of elasticity theory and derived closed form analytical solutions for stresses and displacements in the pipes subjected to internal and/or external pressure.

In China, many large-scale oil, gas, and water transportation projects have been developed recently, extending the use of various kinds of pipe networks and thus increasing

the demands of pipes (Yuan 2010; Chen 2012). Because Chinese topographic conditions are complex, new pipes often need to pass through railways, roads, rivers, mountains, and valleys. Lighter weight pipes are required for the convenience and cost reduction of transportation and installation, especially in areas where transport is a challenge.

Although the cost of GRPM pipes was reduced by incorporating a sand filler layer, the density of GRPM pipes increased. The density of silica sand is approximately 2.6 g/cm^3; thus the density of GRPM pipes with relatively large diameters usually has been greater than 2.0 g/cm^3. Few studies have been conducted on core material other than sand. Bamboo and veneer are biomass materials and widely used in furniture, floor, and building applications. From the point of view of microstructure, bamboo and veneer are natural fiber reinforced composite materials and provide a higher ratio of strength to weight and better toughness than concrete (Li *et al*. 1994; Li 2004). Many investigations have been conducted on the microstructure characteristics, as well as the physical and mechanical properties of bamboo (Huang *et al*. 2005; Jiang *et al*. 2005; Liu 2008). Zhang *et al.* (2005) studied mechanical properties of laminated wood-bamboo composite. Ma *et al.* (2008) designed a bionic columnar structure based on the microstructure of bamboo, and the structure provided a high ratio of strength to weight.

A new design of FRP pipes with bamboo and veneer layers (FRPBV) is presented in this paper. The core layer of the sandwich structure of the FRPBV pipe wall was bamboo and veneer, and the inner and outer layers were FRP. The FRPBV pipes provided an advantage with respect to weight saving and improved mechanical performance.

EXPERIMENTAL

Materials

Veneer (*Pinus sylvestris* var. *mongolica* Litv.) sized 500 × 500 mm with an average thickness of 1.5 mm and a moisture content of 9.8% was used, provided by Big Forestry Wood Industry Co., Ltd., Linyi, China.

Bamboo (treated by spreading and dispersing) sized 100 × 950 mm with an average thickness of 4.5 mm and a moisture content of 7.56% was used, provided by Anji Bamboo & Wood Mechanical Processing Plant, Anji, China.

Glass fiber untwisted yarn was used for filament winding. It was model 12K, had a linear density of 2400 tex, an average diameter of 133 μm, a moisture content of ≤ 0.2%, a hygroscopicity of ≤ 10%, a tensile strength ≥ 1650 MPa, a modulus of elasticity (MOE) of 80 GPa, and a breaking elongation (Elongation is the ratio of elongation length to original length when fiber was stretched to the breaking point) of 4%. It was provided by Taishan Glass Fiber Co., Ltd., Jinan, China.

The adhesive used was unsaturated polyester provided by Changzhou Huake Polymer Co., Ltd., Changzhou, China. Its host was unsaturated polyester resin (UPR), which was a faint yellow transparent liquid. Its viscosity was 350 to 500 cP and its solid content was 59% to 63%.

The accelerant used was cobalt naphthenate provided by Beijing Huixuan Glass Fiber Reinforced Plastics Plant, Beijing, China. It had a cobalt salt content of 9.9%.

The curing agent used was methyl ethyl ketone peroxide provided by Beijing Huixuan Glass Fiber Reinforced Plastics Plant, Beijing, China. Its reactive oxygen content was 9.9%.

The mass ratio of each component was UPR: cobalt naphthenate: methyl ethyl ketone peroxide = 100:0.6:2.

The manufacture and test equipment included a filament winding machine (JC-3000, Harbin Machinery Factory, Harbin, China), a curing oven (NJG101-9, Harbin Machinery Factory), a trim saw (TS300, Harbin Machinery Factory), and a mechanics testing machine (AG-100KN-MO, Japanese Shimadzu [Suzhou] Co., Ltd., Suzhou, China).

Table 1. Main Mechanical Properties of Bamboo, Veneer and Glass Fiber

Material	Moisture Content (%)	Density (g/cm^3)	Tensile Strength (MPa)	Tensile Modulus (GPa)
Bamboo	7.56	0.626	90.35	9.56
Veneer	9.8	0.46	48.35	9.63
Glass Fiber	2	2.56	2350	80

Methods

According to the filament winding method, both the fiber stress and the winding angle (measured from the axial axis of pipe) had important influences on the mechanical properties. Three major factors were considered to conduct orthogonal experiments of the FRPBV pipes: fiber stress, winding angle, and core material. Each factor had three levels (Table 2), resulting in a [$L_9(3^4)$] orthogonal table (Table 3). The three levels of core material considered in this study were veneer, bamboo, and a combination of veneer and bamboo. To guarantee the same thickness of core layer, veneer consisted of six plies, bamboo consisted of two plies, and the combination of veneer and bamboo consisted of three plies of veneer and one ply of bamboo. Each test was repeated three times under the same conditions.

Table 2. The Factors and Levels of Orthogonal Test (L9（3^4)), (A: Fiber stress, B: Winding angle, C: Core material)

Levels	Factors		
	A (N)	*B* (°)	*C*
1	200	15	Veneer
2	250	30	Bamboo
3	300	45	Veneer & bamboo

Table 3. Orthogonal Table (L9（3^4)), (A: Fiber stress, B: Winding angle, C: Core material)

Numbers	Factors		
	A	*B*	*C*
1	1	1	1
2	1	2	2
3	1	3	3
4	2	1	2
5	2	2	3
6	2	3	1
7	3	1	3
8	3	2	1

9	3	3	2

The FRPBV pipes were manufactured by the filament winding method. The process is shown in Fig. 1. The FRPBV pipes were trimmed to specimens for testing as shown in Fig. 2. The length of the specimen was 1000 mm, the inner diameter was 130 mm, and the wall thickness was 10 mm.

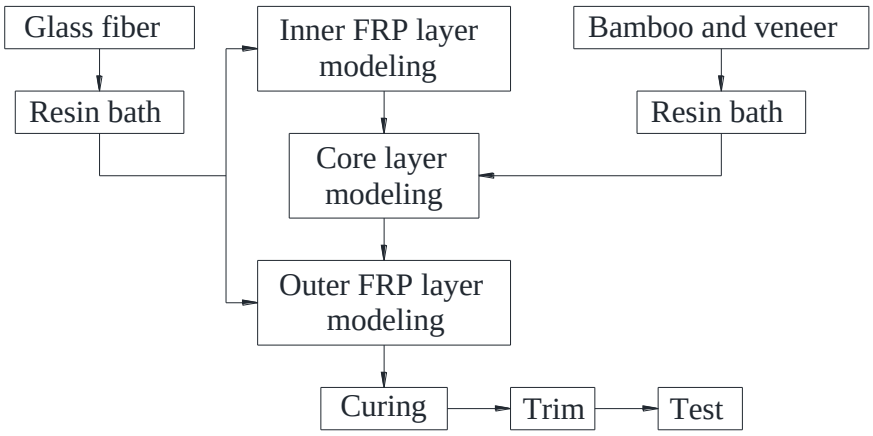

Fig. 1. The manufacturing process of FRPBV pipes

Fig. 2. Specimens of FRPBV pipes

Test Standards

The shearing strength of FRPBV pipes was tested in accordance with Chinese standard GB/T 1458 (2008). The specimen and loading schematic diagrams of the shearing test are shown in Fig. 3. In Fig. 3, L = 50 mm, b = 30 mm, h = 10 mm, R = 65 mm, the radius of the top press block is 3 mm, the distance between the two sliding supports is l = 45 mm, and the loading speed is 1 to 2 mm/min. When testing, the load was evenly and continuously applied until the specimen failure, and the value of shear strength was obtained by Eq.1,

$$\tau_s = \frac{3P_b}{4bh} \quad (1)$$

where τ_s is interlaminar shear strength (MPa), P_b is failure load (N), *b* is the width of specimen (mm), and *h* is the thickness of specimen (mm).

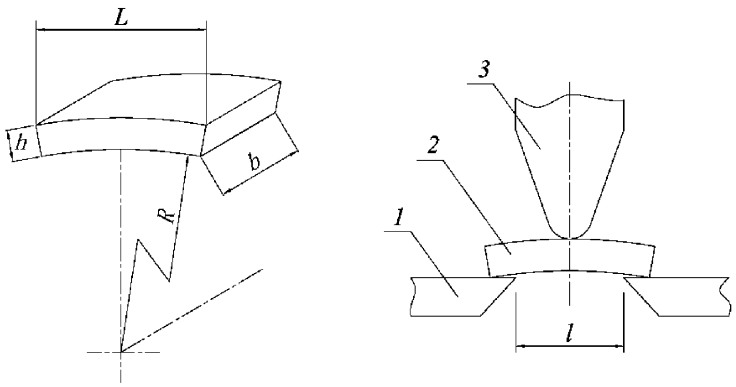

Fig. 3. Specimen and loading schematic diagrams of the shearing test; (1) sliding support, (2) specimen, (3) top press block

The values of pipe stiffness were obtained by Eq. 2 through the parallel-plate loading test (as shown in Fig. 4) according to Chinese standard GB/T 5352 (2005),

$$PS = \frac{F}{\Delta Y} \quad (2)$$

where *PS* is the pipe stiffness (MPa), *F* is the load (N), and ΔY is the deformation under the load.

The specimens were 300 mm in length and 130 mm in diameter, and the size of the plate was 300 × 200 × 6 mm. The loading was gradually applied with the speed of 10 to 12 mm/min. Before testing, specimens were put into a room with a temperature of 23 ± 2 °C and relative humidity of 50 ± 10% for more than 40 h. The parallel-plate loading test was conducted at the same conditions. Values of loading at 5% and 10% deformation were recorded.

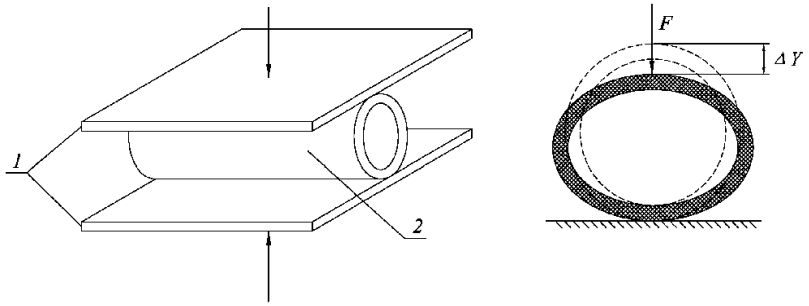

Fig. 4. Schematic diagram of the parallel-plate loading test and description of pipe stiffness; (1) parallel-plates, (2) specimen

RESULTS AND DISCUSSION

Shearing Test

The shearing strength reflected the bonding situation of each layer. The load was evenly and continuously applied until the specimen cracked. The shearing test results, range analysis, and variance analysis are shown in Tables 4, 5, and 6, respectively.

Table 4. Shearing Test Results

Numbers	*A* (N)	*B* (°)	*C*	Shearing Strength (MPa)
1	200	15	Veneer	2.24
2	200	30	Bamboo	3.39
3	200	45	Veneer & Bamboo	2.80
4	250	15	Bamboo	2.86
5	250	30	Veneer & Bamboo	3.82
6	250	45	Veneer	2.53
7	300	15	Veneer & Bamboo	2.58
8	300	30	Veneer	2.36
9	300	45	Bamboo	5.02

A, fiber stress; *B*, winding angle; *C*, core material

Table 5. Range Analysis of Shearing Test

Factors	*A* (N)	*B* (°)	*C*
Mean 1	2.810	2.560	2.377
Mean 2	3.070	3.190	3.757
Mean 3	3.320	3.450	3.067
Range	0.510	0.890	1.380
Priorities		C > B > A	
Optimization scheme		A3 B3 C2	

A, fiber stress; *B*, winding angle; *C*, core material

Computing method of range analysis:

The right column of Shear strength in Table 4 is named as Si, i=1-9, e.g. S1=2.24, S2=3.39, and so on. Table 5 is obtained based on Table 4. The rows of Mean 1, 2, 3 in Table 5 are shear strength average of factors A, B, C at level 1, 2, 3 separately. Mean 1A = (Si+Sj+Sk)/3, Si, Sj, Sk are shear strength of factor A at level 1 in Table4. For example, level 1 of factor A is 200, so Mean 1A = (S1+S2+S3)/3. Similarly, level 1 of factor B is 15, Mean 1B = (S1+S4+S7)/3; level 1 of factor C is veneer, Mean 1C = (S1+S6+S8)/3, and so on.

RangeA = max(mean1A,mean2A,mean3A) — min(mean1A,mean2A,mean3A), and so on.

Table 5 shows that the order of the influence of factors was as follows: C > B > A; the core material was the most influential factor on the shearing strength of the pipe. Although the influence on the shearing strength of the three factors in Table 6 were all negligible, the order of the factors' influence, from the point of view of the values of *F*, remained C > B > A, the same as the range analysis of Table 5.

Shearing strength increased as fiber stress and winding angle increased from mean values in Table 5. The increase of fiber stress and winding angle increased the pressure on the core material, which was conducive to the effects of glue.

Table 6. Variance Analysis of Shearing Test

Factors	Sum of Square of Deviation	Degree of Freedom	F	Significance
A	0.390	2	0.339	--
B	1.257	2	1.092	--
C	2.857	2	2.482	--
Error	3.450	6		

$F_{0.01}(2,6) = 10.92$; $F_{0.05}(2,6) = 5.14$; $F_{0.1}(2,6) = 3.46$
A, fiber stress; *B*, winding angle; *C*, core material

Almost all fractures in test specimens occurred between the FRP layer and the veneer layer, or between the ply and the ply of veneer. The frequency of these fracture locations indicated that the veneer was not well glued to the FRP or to itself. Two reasons may have caused the fractures. One is that the fiber stress may have been too low for veneer gluing. The pressure needed to manufacture veneer for plywood is approximately 1.5 MPa, but the highest pressure that the winding machine could provide was only 0.5 MPa. The other reason is that the resin content of veneer may have been too high. Although *Pinus sylvestris* veneer had an advantage over other fast growing wood in terms of mechanical properties, its high resin content produced a negative effect on gluing. This reason also explained why bamboo glued better than veneer at the same conditions.

The optimized experimental scheme was obtained from range analysis and variance analysis of the shearing tests. Namely, the fiber stress was 300 N, the winding angle was 45°, and the core material was bamboo.

Parallel-Plate Loading Test

The pipe stiffness indicates the resistance of the pipe to external transverse loading. The importance of this physical characteristic becomes more pronounced when buried or underground pipe applications are sought (Rafiee and Reshadi 2014). The parallel-plate loading test results are shown in Table 7.

Table 7. Parallel-Plate Loading Test

Numbers	*A*(N)	*B*(°)	*C*	Pipe Stiffness (MPa)	
				5% Deformation	10% Deformation
1	200	15	Veneer	0.390	0.263
2	200	30	Bamboo	1.600	1.347
3	200	45	Veneer & Bamboo	1.967	0.967
4	250	15	Bamboo	1.396	0.550
5	250	30	Veneer & Bamboo	0.936	0.697
6	250	45	Veneer	1.040	0.863
7	300	15	Veneer & Bamboo	0.733	0.484
8	300	30	Veneer	0.740	0.552
9	300	45	Bamboo	1.527	0.727

A, fiber stress; *B*, winding angle; *C*, core material

(a) (b)

Fig. 5. Pipes under parallel-plate loading with (a) 5% deformation and (b) 10% deformation

The entire process of the parallel-plate loading test was observed. Loading was increased until the deformation of pipe reached 5%. No fractures were observed within each layer, but some white lines and grids along the direction of the fibers were found on the surfaces of the outer and inner layers of pipe (shown in Fig. 5a), a sign that the fiber was going to separate from the resin. As the loading continued to increase, delamination between the core layer and the FRP layer was observed. When the deformation of the pipe reached 10%, depression, cracks, and separation between layers occurred, as shown in Fig. 5b.

Table 8. Range Analysis of Parallel-Plate Loading Test

Factors		*A*(N)	*B*(°)	*C*
5% Deformation	Mean 1	1.319	0.840	0.723
	Mean 2	1.124	1.092	1.508
	Mean 3	1.000	1.511	1.212
	Range	0.319	0.671	0.785
	Priorities		*C* > *B* > *A*	
	Optimization scheme		A1 B3 C2	
10% Deformation	Mean 1	0.859	0.432	0.560
	Mean 2	0.703	0.866	0.874
	Mean 3	0.588	0.852	0.716
	Range	0.271	0.434	0.314
	Priorities		*B* > *C* > *A*	
	Optimization scheme		A1 B2 C2	

A, fiber stress; *B*, winding angle; *C*, core material
Computing method of range analysis is as same as Table 5.

Table 9. Variance Analysis of Parallel-plate Loading Test

Factors		Sum of Square of Deviation	Degree of Freedom	F	Significance
5% Deformation	*A*	0.155	2	0.420	--
	B	0.690	2	1.868	--
	C	0.942	2	2.551	--
	Error	1.110	6		
10% Deformation	*A*	0.111	2	0.515	--
	B	0.364	2	1.688	--
	C	0.148	2	0.686	--
	Error	0.650	6		

$F_{0.01}(2,6) = 10.92$; $F_{0.05}(2,6) = 5.14$; $F_{0.1}(2,6) = 3.46$
A, fiber stress; *B*, winding angle; *C*, core material

The range analysis and variance analysis of parallel-plate loading test are shown in Tables 8 and 9, respectively. At 5% deformation, the order of the factors' influence was *C* > *B* > *A*, and, at 10% deformation, and the order of influence was *B* > *C* > *A*. Considering the deformation of specimen with loading, it was assumed that core material was the most influential factor on pipe stiffness. At 5% deformation, no fractures were found in the layers of the specimen; thus, the results of the 5% deformation in Table 8 and Table 9 were actual reflections of the mechanical properties of pipes. At 10% deformation, depression, cracks, and separation between layers were observed in the specimen, and the function of

pipe partially failed. Thus, the analysis on the 10% deformation in Table 8 and Table 9 was not exactly accurate.

The optimized experimental scheme of the parallel-plate loading test was obtained from range analysis and variance analysis. The fiber stress was 200 N, the winding angle was 30°, and the core material was bamboo.

The final optimization experimental scheme of FRPBV pipes was obtained considering the analysis of shearing and parallel-plate loading tests. The fiber stress was 300 N, the winding angle was 30°, and the core material was bamboo.

The largest fiber stress that the machine could provide, 300 N, was chosen because that greater fiber stress benefitted the bonding of layers. According to the investigation of Krishnan (2015), each winding angle dominates a different optimum pressure loading condition. Thus, the winding angle was chosen considering the actual loading condition of pipes. The angle of 30° was chosen because a specimen with a winding angle of 30° sustained a longer time before failure under loading than those with other winding angles. Bamboo was chosen as the core material according to analysis of shearing and parallel-plate loading tests.

The FRPBV pipes were manufactured according to the final optimization experimental scheme, and shearing and parallel-plate loading tests were carried out. The results showed that the shearing strength was 4.13 MPa, the pipe stiffness was 2.21 MPa, and the average density was 0.94 g/cm^3, approximately half the density of GRPM pipes.

CONCLUSIONS

1. A new design of FRPBV pipes was presented. Orthogonal experiments with three factors, namely, fiber stress, winding angle, and core material, were carried out.
2. Range analysis and variance analysis of orthogonal experiments were conducted to investigate the effects of fiber stress, winding angle, and core material on the mechanical performance of FRPBV pipes subjected to shearing and parallel-plate loading tests.
3. The new design of FRP pipes with a bamboo and veneer layer was feasible, and core material was the most influential factor on mechanical performance. The FRPBV pipe had better mechanical performance with a fiber stress of 300 N, a winding angle of 30°, and the core material of bamboo. The average density of FRPBV pipes was 0.94 g/cm^3, approximately half of that of GRPM pipes. It provided an advantage on weight saving and mechanical performance improvement and showed a great application potential in future.
4. Two reasons may have caused the veneer to adhere poorly to the FRP or itself by glue. One reason is that the fiber stress that the winding machine provided was too low for veneer gluing. The other is that the high resin content of *Pinus sylvestris* veneer produced a negative effect on gluing.
5. The FRPBV pipes were manufactured by winding machine for FRP pipes. Technology parameters that the winding machine could provide did not achieve requirements of veneer and bamboo gluing. Machine and process for FRPBV pipes should be studied and improved in future work.

ACKNOWLEDGMENTS

The authors are grateful for the support of the Fundamental Research Funds for the Central Universities (NO. BLX2015-19), MOE Key Laboratory of Wooden Material Science and Application, Beijing Key Laboratory of Wood Science and Engineering and Beijing Composites Material Co., Ltd.

REFERENCES CITED

Arjomandi, K., and Taheri, F. (2012). "Bending capacity of sandwich pipes," *Ocean Engineering* 48, 17-31. DOI: 10.1016/j.oceaneng.2011.09.014

Chen, J. Z. (2012). "Development report of filament winding products," *Fiber Reinforced Plastics/Composites* (3), 94-96. DOI: 10.3969/j.issn.1003-0999.2012.03.021.

GB/T 1458 (2008). "Test method for mechanical properties of ring of filament-winding reinforced plastics," Standardization Administration of China, Beijing, China.

GB/T 5352 (2005). "Fiber-reinforced thermosetting plastic composites pipe – Determination for external loading properties by parallel-plate loading," Standardization Administration of China, Beijing, China.

Huang, S. X., Ma, L. N., Shao, Z. P., and Zhou, X. H. (2005). "Relationship between microstructure characteristics and mechanical properties of moso-bamboo," *Journal of Anhui Agricultural University* 32(2), 203-206. DOI: 10.13610/j.cnki.1672-352x.2005.02.017.

Jiang, Z. H., Chang, L., Wang, Z., and Gao, L. (2005). "Physical and mechanical properties of glued structural laminated bamboo," *China Wood Industry* 19(4), 22-30. DOI: 10.3969/j.issn.1001-8654.2005.04.007.

Kaveh, A., and Farid, T. (2011). "The influence of intra-layer adhesion configuration on the pressure capacity and optimized configuration of sandwich pipes," *Ocean Engineering* 38, 1869-1882. DOI: 10.1016/j.oceaneng.2011.06.006.

Kong, F. X., and Kong Q. B. (2010). "The practical design of cure schedule for filament winding composites I," *Fiber Composites* (4), 22-29. DOI: 10.3969/j.issn.1003-6423.2010.04.005.

Kong, F. X., and Kong Q. B. (2011). "The Practical design of cure schedule for filament winding composites II," *Fiber Composites* (1), 11-20. DOI: 10.3969/j.issn.1003-6423.2011.01.003.

Krishnan, P., Majid, M. S. A., Afendi, M., Gibson, A. G., and Marzuki, H. F. A. (2015). "Effects of winding angle on the behaviour of glass/epoxy pipes under multiaxial cyclic loading," *Materials and Design* 88, 196-206. DOI: 10.1016/j.matdes.2015.08.153

Li, F., Zhao, Q. L., Xu, K., and Zhang, D. D. (2015). "Experimental tests on the composite foam sandwich pipes subjected to axial load," *Appl. Compos. Mater.* 22, 669-691. DOI: 10.1007/s10443-014-9430-3.

Li, H. Q. (2004). "Bionic fiber reinforced composites," *Technical Textiles* (8), 1-5. DOI: 10.3969/j.issn.1004-7093.2004.08.001.

Li, S. H., Fu, S. Y., and Zhou, B. L. (1994). "A natural composite material——bamboo," *Chinese Journal of Materials Research* 8(2), 188-192.

Liu, Y. D., Gui, R. Y., Yu, Y. M., Chen, C. J., and Fang, W. (2008). "A preliminary study on the physical and mechanical properties of different provenances of Moso bamboo," *Journal of Bamboo Research* 27(1), 50-54. DOI: 10.3969/j.issn.1000-6567.2008.01.010.

Ma, J. F., Chen, W. Y., Zhao, L., and Zhao, D. H. (2008). "Bionic design of columnar structure based on microstructure of bamboo," *Journal of Machine Design* 25(12), 50-53. DOI: 10.13841/j.cnki.jxsj.2008.12.010.

Mehmet, E. D., and Ramazan, K. (2012). "Seawater effect on impact behavior of glass-epoxy composite pipes," *Composites Part B: Engineering* 43(3), 1130-1138. DOI: 10.1016/j.compositesb.2011.11.006

Qin, R. Y. (1996). "Processing parameters analysis for RPM pipes," *Fiber Reinforced Plastics/Composite* 2, 30-33.

Rafiee, R., and Amini, A. (2015). "Modeling and experimental evaluation of functional failure pressures in glass fiber reinforced polyester pipes," *Computational Materials Science* 96(B), 579-588. DOI: 10.1016/j.commatsci.2014.03.036

Rafiee, R., and Reshadi, F. (2014). "Simulation of functional failure in GRP mortar pipes," *Composite Structures* 113,155-163. DOI: 10.1016/j.compstruct.2014.03.024

Sburlati, R., and Kashlatyan, M. (2016). "Elasticity analysis of sandwich pipes with functionally graded interlayers," *European Journal of Mechanics A/Solids* 59, 232-241. DOI: 10.1016/j.euromechsol.2016.03.012.

Wang, Z., Deng, J. L., Wang, J. H., and Ding, A. X. (2014). "Ring stiffness finite element analysis and application of GRP pipes," *FRP/CM* (11), 16-20.

Xu, J. Z., Qiao, M., You, B., and Wang, X. Y. (2009). "Research of in-situ modeling process for fiber winding composite shell," *Material Science & Technology* 17(2), 191-194.

Yang, H. (2008). "Numerical simulation of the cure process of the filament-wound composites," *Journal of Mechanical Strength* 30(2), 250-254. DOI: 10.16579/j.issn.1001.9669.2008.02.016.

Yang, J. M., Hu, Z. Y., and Li, X. C. (2013). "Quality control of glass fiber reinforced plastics mortar pipe with definite-length-winding," *Fiber Reinforced Plastics/Composites* 5, 60-61. DOI: 10.3969/j.issn.1003-0999.2013.05.013.

Yuan, L. (2010). "On design for large-span water supply pipes," *ShanXi Architecture* 36(3), 200-202. DOI: 10.3969/j.issn.1009-6825.2010.03.124.

Zhang, X. D., Li, J., Wang, Q. Z., and Zhu, Y. X. (2005). "Mechanical property prediction of laminated wood-bamboo composite and analysis," *Journal of Nanjing Forestry University (Natural Sciences Edition)* 29(6), 103-105. DOI: 10.3969/j.issn.1000-2006.2005.06.026.

Article submitted: October 25, 2016; Peer review completed: December 12, 2016; Revised version received and accepted: February 12, 2017; Published: February 21, 2017.
DOI: 10.15376/biores.12.2.2699-2710